Estimating basement faults with vertical slips using gravity inversion in onshore Almada Basin, Brazil

Valéria Cristina F. Barbosa (*), LNCC, Paulo Tarso L. Menezes, DGAP/FGEL/UERJ, and João Batista C. Silva, UFPA.

Abstract

We illustrate that the depth imaging of the fault plane may be obtained using gravity data. Our approach is based on a method that enhances the estimated relief resolution as compared with methods incorporating smoothness constraints. Our results using gravity data from Almada Basin, Brazil, produced an interpretative depth image of the faults compatible with the available seismic data interpretation.

Introduction

Faults are features particularly difficult to be detected from gravity data only. The delineation of faults in depth using the vertical component of the gravity data is, usually, very poor. In this case, the very existence of faults might, at most, be guessed if the fault has a sharp discontinuity with large vertical throw. Commonly, the fault detection and the structural tectonic analysis are performed in a semiquantitative way, by some processing techniques applied to gridded data (e.g., the amplitude of the analytic signal and the first and second vertical derivatives anomaly maps). The result is an interpretative image of the fault, i.e., a map displaying the fault traces at Earth's surface.

On the other hand, the delineation of the faults in depth from gravity data still remains a vexed problem. A severe drawback in gravity interpretation is the presence of faults with small vertical slip. This may become a hindrance if the geological setting is composed by a sequence of small step faults closely spaced. This is one of the reasons why the depth imaging of the fault-plane geometry is often performed mainly via seismic data interpretation. The majority of gravity interpretation methods yield good results for smooth models; however, they are unable to recover blocky structures such as non-smooth basement relief.

In this study we present an interpretation of the three-dimensional onshore Almada basement's topography obtained by applying Barbosa et al.'s (1997) method to the gravity anomaly. Besides, we explore the potential use of gravity data to detect and delineate faults in the onshore portion of Almada Basin (AB), Brazil (Figure 1). This last goal is attained using the Barbosa et al.'s (1999) method that enhances the estimated relief resolution as compared with methods incorporating smoothness constraints (e.g., Barbosa et al., 1997).

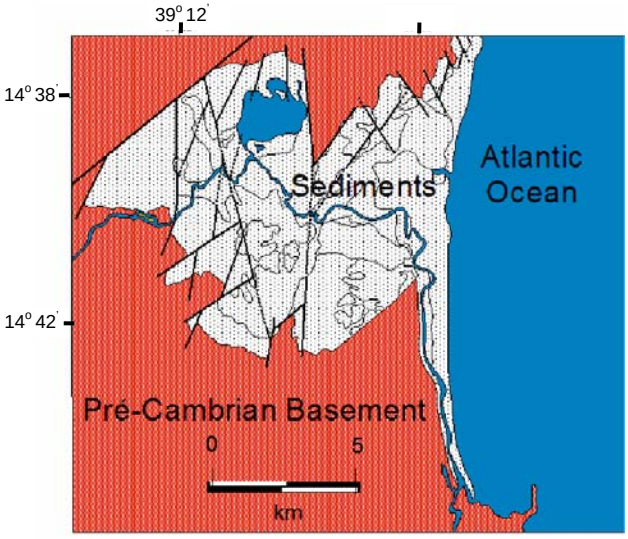

Figure 1 – Location of the onshore portion of Almada Basin, Brazil, with main mapped faults.

Method

The Camamu-Almada Basin is located in the northern portion of the Brazilian continental margin, being limited to the north by the Recôncavo Basin and to the south by the Jequitinhonha Basin. The tectonic and sedimentary evolution are related to the geodynamic processes that conditioned the formation of the South Atlantic Ocean (Ponte and Asmus, 1978), with three main sedimentary sequences linked to the main tectonics stages: pre-rift, rift and post-rift (Ponte and Asmus, 1978). The onshore portion of the Camamu-Almada Basin (Figure 1) was object of an exploratory program in the 1970s, with a few 2D seismic lines and five drilled boreholes, one being considered sub-commercial for oil (Brunh and Moraes, 1989).

The gravity dataset used in this study contains 1100 gravity points from a public domain dataset made available as Bouguer anomaly by ANP (the Brazilian Petroleum Agency) and 220 new gravity stations, collected by the authors to fill in the preexistent gaps. The Bouguer anomaly map, obtained after the processing corrections, is shown in the Figure 2. A strong regional gravity effect, possibly produced by the crust-mantle interface, is clearly evidenced by a long-wavelength north-south trending data. This behavior is consistent with the previous knowledge of the Moho in the region. The gravity highs at the southeastern and northeastern

corners are the main anomalies associated to basement outcrops known as the Itacaré and Olivença Highs, respectively. The regional effect caused by deep sources and these gravity highs mask the expected gravity low associated with the Almada Basin at point AB, where the sediments outcrop.

Figure 3 shows the Bouguer gravity anomaly over onshore Almada Basin corrected for deeper crustal effects. The correction consisted of subtracting from the original observations (Figure 2) a second-degree polynomial fitted to the gravity data by a robust method (Beltrão et al., 1991). This method reduces the influence of the residual component in the fitted regional. The second degree was selected because it leads to a negative residual anomaly that best coincides with the Almada Basin borders (Figure 3). The second-degree regional anomaly (Figure 4) reveals an eastward crustal thinning whose strike, approximately in the north-northeast direction is consistent with its geodynamic origin: the Mesozoic breakup of Gondwana and the opening of the South Atlantic Ocean (Ponte and Asmus, 1978).

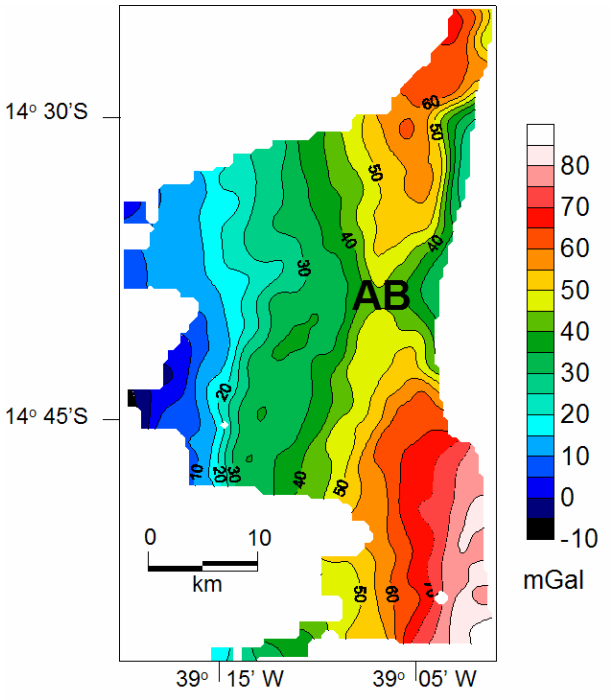

Figure 2 - Bouguer anomaly map from onshore Almada Basin (AB) and adjacent regions.

Inversion Results

Almada basement relief estimates

The three-dimensional onshore Almada basement topography was obtained by applying Barbosa et al.'s (1997) method to the gravity anomaly shown in Figure 3. This method estimates the basement depths at discrete points assuming that the density contrast between the sediments and the basement is constant and known. By minimizing a first finite–difference approximation of the basement depths, Barbosa et al.'s (1997) method favors a relatively flat solution and implicitly introduces prior information that the basement relief is overall smooth. Furthermore, this method allows incorporating the prior knowledge about the basement depth provided by boreholes by constraining the estimated depths to be close to the true depths (in the least-squares sense) at isolated points where the depths are known.

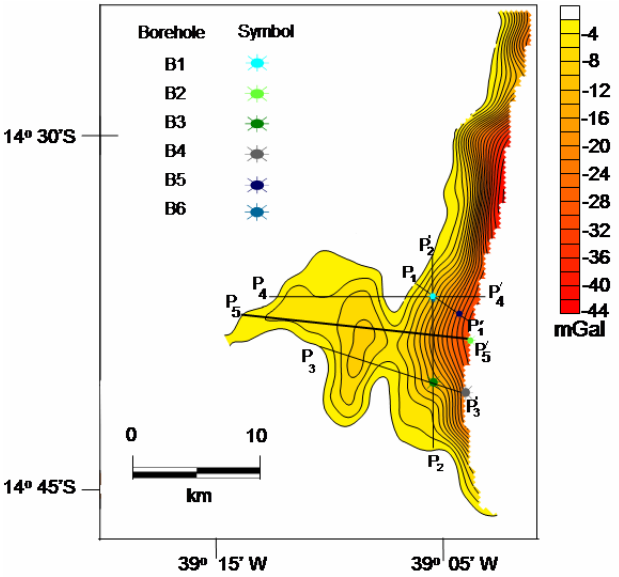

Figure 3 - Bouguer anomaly map from onshore Almada Basin, corrected for the effect of an eastward crustal thinning. B1-B6 are boreholes. $P_1P'_1$, $P_2P'_2$, $P_3P'_3$, $P_4P'_4$ and $P_5P'_5$ are gravity profiles shown in Figures 6-10, respectively.

We presumed that the Bouguer gravity anomaly, shown in Figure 3, is produced by the onshore Almada's basement relief. These data were interpolated at a regular grid spacing of 0.4 km in both north-south and east-west directions. From the available geological information, we assumed a constant density contrast of -0.4 g/cm3 between the sediments and the basement. Borehole information about the basement depth at six points were used (B1–B6 in Figure 3) whose locations are given in Table 1.

The estimated Almada basement relief by Barbosa et al.'s (1997) method (Figure 5) was obtained at 5085 discrete points producing an acceptable Bouguer anomaly fitting (not shown). Figure 5 shows that three features of the Almada basement topography are apparent: (1) the structural low (L1); (2) terraces (T1 and T2); and (3) the sloping area (S1). The low L1 is depicted as a shallow isolated fault-bounded subbasin where northeast-trending faults circumscribe a single elongated depocenter having a maximum depth of 0.5 km. The slope gradient in the area S1 is variable, ranging from a low slope gradient, close to low L1 where the estimated average dip angle is around 15°, to high-angle fault, in the northernmost basin border where the estimated average dip angle is around

66°. Despite the substantial change in the average dip angle at S1, the estimated relief shows a constant east-dipping slope. Having isolated the subbasin L1 from the sloping area S1, we note a low gradient area representing a narrow terrace T1. The second terrace T2 is inferred from the low gradient area located at the westernmost portion of the Almada Basin. Table 2 shows the observed and estimated depths at boreholes B1-B6. The "mis-tie" at borehole B4, located at the border of the data window (Figure 5), is an edge effect because Barbosa et al.'s (1997) method constraints the basement relief to be flat and this premise is violated at the data window border but not at the center of the basin.

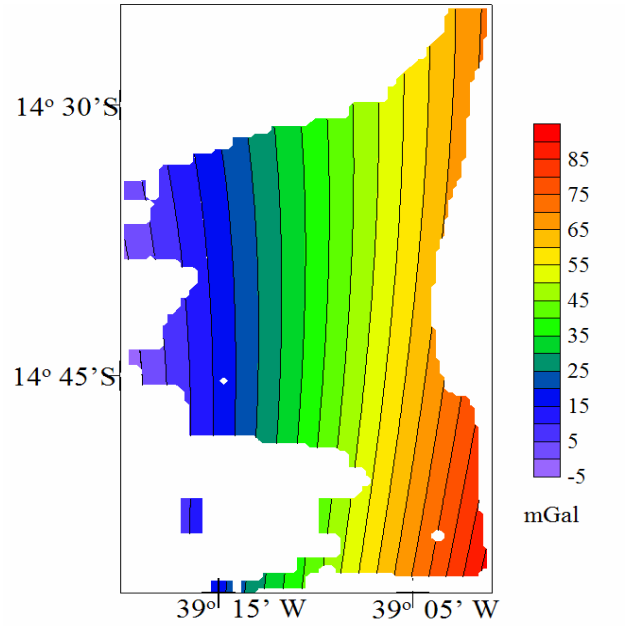

Figure 4 - Regional gravity anomaly using a robust second-degree polynomial fitting of the gravity data shown in Figure 2.

The inversion result (Figure 5) shows that the Almada Basin framework is strongly controlled by several faults. It is consistent with the geological information reported by Netto and Sanches (1991) that the Almada Basin is a fault-bounded sedimentary basin delimited by the northeast-trending Itabuna-Itaju do Colônia Shear Zone represented in the area by Serra Pilheira Fault. Some known faults are revealed in Figure 5. Two northeast-trending faults that control the Almada basin borders are noticeable: Serra Pilheira Fault (SPF) and Marron Fault (MF). In agreement with the geological evidence, we inferred, in the northernmost Almada Basin border, the north-south-trending Aritaguá Fault (AF). The subtle distortion of the contour lines near the borehole B1, suggests the presence of a northwest-trending faults, apparently younger than the Aritaguá Fault, which resemble to be arranged as an en-echelon fault zone. The Apipique (ApF) and Piábas (PF) Faults circumscribe the shallow subbasin L1, and they are inferred from the gradient change around the contour line 0.3 km.

Borehole	Latitude	Longitude	Depth (km)
B1	14° 37' 0.0'' S	39° 05' 30.0'' W	0.396
B2	14° 38' 39.1'' S	39° 03' 52.9" W	1.464
B3	14° 40' 29.1'' S	39° 05' 31.3'' W	0.493
B4	14° 40' 56.7''S	39° 03' 56.2'' W	1.650
B5	14° 37' 41.1''S	39° 04' 17.3'' W	1.245
B6	14° 37' 9.7'' S	39° 05' 27.3'' W	0.418

Table 1. Geographic coordinates of six boreholes (B1-B6) and the corresponding depths to the basement in Almada Basin.

Borehole	Observed (km)	Estimated (km)	Mis-tie (km)
B1	0.396	0.280	0.116
B2	1.464	1.572	0.108
B3	0.493	0.464	0.029
B4	1.650	1.283	0.367
B5	1.245	1.174	0.071
B6	0.418	0.378	0.040

Table 2 - Almada Basin - Observed and estimated basement depths at six boreholes (B1-B6), and residual depths (absolute differences between the observed and estimated depths).

Faults enhancement

As we pointed out before, Barbosa et al.'s (1997) method imposes an overall smoothness on the basement topography. In this way, using this method we did not expect to estimate high-angle faults in the basement relief. In fact, Figure 5 shows an estimated relief essentially smooth. The interpreted faults (AF, MF, PF, SPF and ApF) were just inferred from a subtle gradient changes in the estimated relief. This result suggests that Barbosa et al.'s (1997) method should be better applied to intracratonic sag basins where the basement relief is essentially smooth and without fault scarps. From the geological viewpoint, these attributes do not reflect the structural framework of the Almada Basin that is strongly controlled by two fault systems, northeast- and northwest-trending faults, both implanted during Early Cretaceous South Atlantic rifting. It is clear that by choosing the Barbosa et al.'s (1997) method does not provide valuable deeper information about fault morphology. Therefore, it is reasonable to use an inversion method suitable for interpreting a faulted basement. For this reason, we explore the potential use of the Barbosa et al.'s (1999) gravity inversion to produce an in depth image of the Almada basement faults.

Barbosa et al.'s (1999) gravity inversion improves the estimated basement relief resolution allowing the mapping of discontinuities which are not trivially inferred from the gravity anomaly just from inspection. This method establishes, via an iterative algorithm, that the estimated basement relief be overall smooth, but may present local abrupt discontinuities. Starting from the Barbosa et al.'s (1997) solution, which imposes a maximum spatial smoothness on the estimated basement relief, Barbosa et al.'s (1999) method updates the basement relief estimate by minimizing the norm of the weighted first-order derivatives of the basement depths where the weights are automatically updated to, at each iteration, enhance any discrepancy between adjacent depths that have been detected at the initial solution. In this way, along the successive iterations, the maximum smoothness information is relaxed allowing the estimate of a non-smooth features on the basement relief. Other constraints are used to compensate for the decrease in solution stability due to the relaxation of the maximum smoothness. According to Barbosa et al. (1999) this method is referred to as weighted smoothness inversion and shows a good resolution in defining both the discontinuities and the low gradient areas of the basement relief, indicating the adequacy of the method for interpreting gravity data from rift basins.

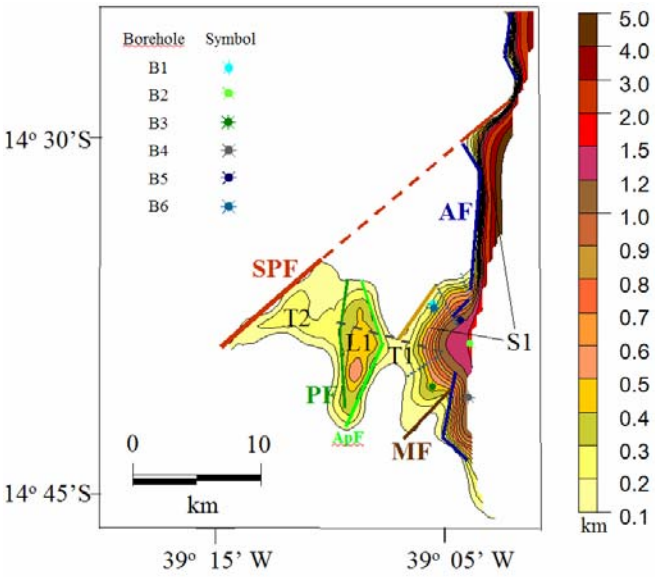

Figure 5- Onshore Almada Basin, Brazil. Estimated basement relief using Barbosa et al.'s (1997) inversion method. B1-B6 are the boreholes. Color thick lines are representing the interpreted trace of the following faults: Serra Pilheira Fault (SPF), Marron Fault (MF), Aritaguá Fault (AF). Apipique Fault (ApF), and Piábas Fault (PF). The Interpreted structural features are: subbasin (L1), terraces (T1 and T2), and sloping area (S1).

We performed several 2D inversions of the Bouguer anomaly of Almada Basin using the weighted smoothness method. We prefer a two-dimensional inversion because we could not resolve such small faults with 3D inversion. Specifically, we selected 5 gravity profiles P1-P5 (see location in Figure 3) which were digitized directly from the non gridded data of Figure 3. The results are shown in Figures 6-9, where the observations are in dots and the fitted gravity anomalies using the weighted smoothness method are in solid lines and the estimated depths to the Almada's basement are in dashed lines. In these results all anomaly fittings are equally acceptable. We assumed a constant level base varying from zero to 1.5 mGal and a constant density contrast of -0.4 $\pm$ 0.5 g/cm3 between the sediments and the basement. Existing borehole data were employed as a mathematical constraint.

Figures 6a-c, 7a-c, and 8a-c show the inversion results of the gravity anomalies profiles $P_1P'_1$, $P_2P'_2$ and $P_3P'_3$, respectively. Specifically, The Figures 6b, 7b, and 8b show the estimated basement relief (dashed line) using Barbosa et al.'s (1997) method. These results show the ability of the Barbosa et al.'s (1997) method to detect the main structural features of the Almada Basin such as the structural low L1, the terrace T1 and the sloping area S1 in Figure 8b. However, this method fails to detect fine structures such as discontinuities caused by small step faults. Rather, the weighted smoothness inversion (dashed line, in Figures 6c, 7c, and 8c) show good resolution in defining both the discontinuities with small or large slips and the low gradient areas of the Almada basement relief. These results demonstrate the ability of the Barbosa et al.'s (1999) method to map the following features.

The first is an isolated high-angle fault, in Figure 6c, coinciding with Aritaguá Fault (AF). The second feature is a sequence of faults, such as those shown in Figure 7c where clearly map two faults: MF correlated with the known Marron Fault and UF not correlated with any known geological fault. The Third feature is a sequence of alternating terraces and structural lows close to each other, such as those shown in Figure 8c where the estimated relief displays: (1) the terraces T1, and T2, both also mapped using Barbosa et al.'s (1997) inversion (see Figure 5); (2) structural lows L1, isolated by the Apipique (ApF) and Piábas (PF) Faults, and L2, in the interval $x \in$ [9 km, 11 km], which does not coincide with any known geological feature; and (3) high-angle fault with large vertical displacement coincides with Aritaguá Fault (AF). When compared with Barbosa et al.'s (1997) estimated reliefs (Figures 6b, 7b and 8b), the estimated reliefs using weighted smoothness inversion (Figures 6c, 7c and 8c) produce a superior performance where a system of faults is expected to occur. Despite being substantially different, both inversions yield acceptable anomaly fits. Figures 6a-8a show the fitted anomalies (solid lines) produced by weighted smoothness inversion.

For comparison, we show in Figures 6d, 7d and 8d the Netto and Sanches' (1991) geological cross-section interpretation based on two-dimensional seismic reflection and borehole data of the profiles $P_1P'_1$, $P_2P'_2$ and $P_3P'_3$, respectively. We note that the estimated reliefs using Barbosa et al.'s (1997) method (Figures 6b-8b) are consistent with the previous geological interpretation presented by Netto and Sanches (1991). However, Barbosa et al.'s (1997) method favors solutions displaying an overall smoothness on the estimated relief. On the other hand, Barbosa et al.'s (1999) method favors

solutions exhibiting reliefs with sharp discontinuous (Figures 6c-8c) being quite close to the Netto and Sanches' (1991) seismic interpretation.

Figures 9a and 9c show the gravity anomalies (dots) along the profiles $P_4P'_4$ and $P_5P'_5$, respectively. The weighted smoothness inversion results (dashed lines) of profiles $P_4P'_4$ and $P_5P'_5$, are shown in Figures 9b and 9d, respectively. Since these profiles are approximately parallel, they detect the same main geological features, such as, the terrace T2 and the structural low L1. The detection of the fault AF as a high-angle fault in both profiles, indicates the method's ability to map this geological feature that could not have been detected just by inspecting the gravity data. The fitted anomalies (solid lines) of profiles $P_4P'_4$ and $P_5P'_5$ are shown in Figures 9a and 9c, respectively.

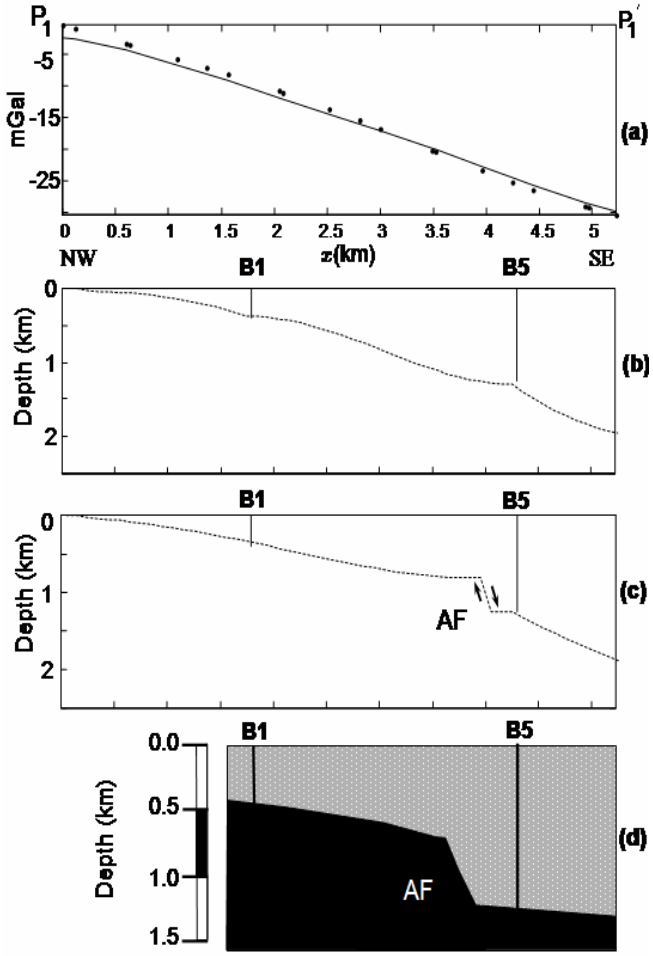

Figure 6 – Profile $P_1P'_1$. (a) Observed (dots) and fitted (solid line) Bouguer anomalies using weighted smoothness inversion along profile $P_1P'_1$ whose location is shown in Figure 3. (b) Estimated Almada basement relief using Barbosa et al.'s (1997) method (dashed line). (c) Estimated Almada basement relief using weighted smoothness inversion (dashed line). (d) Netto and Sanches's (1991) geological cross-section seismic interpretation. Both inversions used the basement depths information provided from boreholes B1 and B5. AF – Aritaguá Fault.

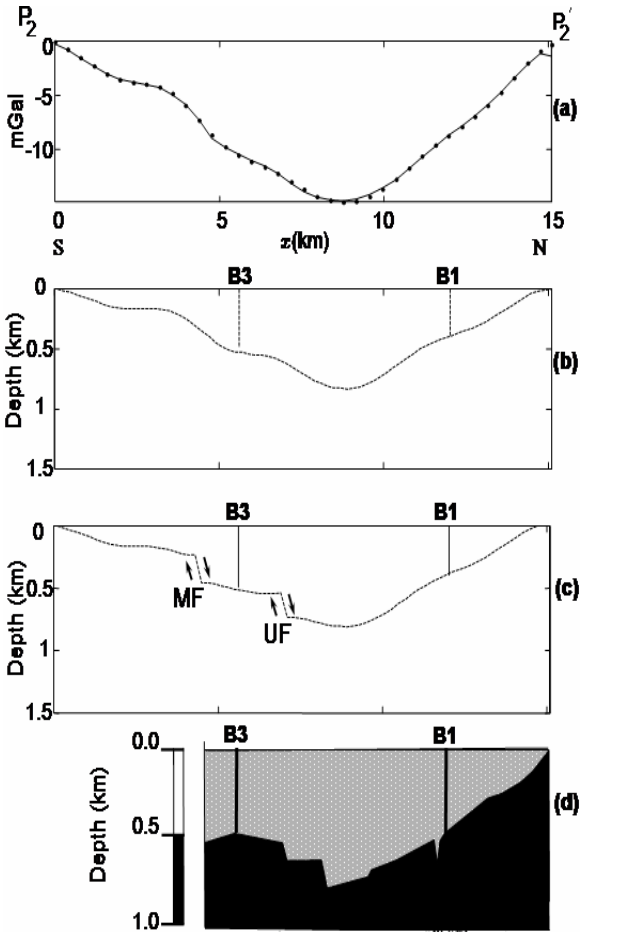

Figure 7 – Profile $P_2P'_2$. (a) Observed (dots) and fitted (solid line) Bouguer anomalies using weighted smoothness inversion along profile $P_2P'_2$ whose location is shown in Figure 3. (b) Estimated Almada basement relief using Barbosa et al.'s (1997) method (dashed line). (c) Estimated Almada basement relief using weighted smoothness inversion (dashed line). (d) Netto and Sanches's (1991) geological cross-section seismic interpretation. Both inversions used the basement depths information provided from boreholes B1 and B3. MF – Marron Fault; UF – fault not correlated with any known geological fault.

Conclusions

We presented a potential application of gravity data to detect and delineate faults in the basement relief of a rift basin. To this end, we employed a weighted smoothness inversion method to gravity data of the onshore portion of Almada Basin, Brazil. Several structural features were evidenced such as sequences of small step faults, or alternate sequences of terraces and structural lows very close to each other, or isolated faults with small or large vertical slips are common. Our results showed a close agreement with previous in depth fault imaging using seismic interpretation, demonstrating the gravity inversion ability to map faults of the Almada's Basin relief.

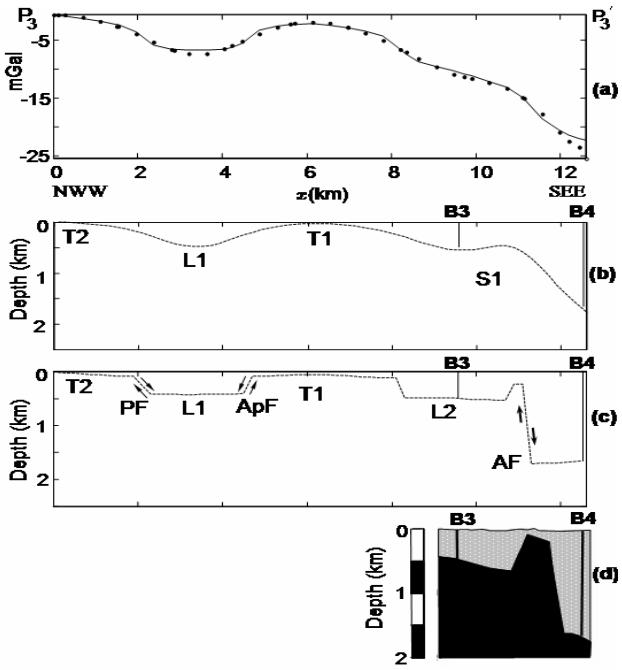

Figure 8 – Profile $P_3P'_3$. (a) Observed (dots) and fitted (solid line) Bouguer anomalies using weighted smoothness inversion along profile $P_3P'_3$ whose location is shown in Figure 3. (b) Estimated Almada basement relief using Barbosa et al.'s (1997) method (dashed line). (c) Estimated Almada basement relief using weighted smoothness inversion (dashed line). (d) Netto and Sanches's (1991) geological cross-section derived from seismic interpretation. Both inversions used the basement depths information provided from boreholes B3 and B4. ApF - Apipique Fault; PF – Piábas Fault; AF – Arituaguá Fault; L1 and L2 – structural lows; T1 and T2 – terraces.

References

Barbosa, V. C. F., J. B. C Silva, and W. E. Medeiros, 1997, Gravity inversion of basement relief using approximate equality constraints on depths: Geophysics, 62, 1745-1757.

Barbosa, V. C. F., J. B. C Silva, and W. E. Medeiros, 1999, Gravity inversion of a discontinuous relief stabilized by weighted smoothness constraints on depth: Geophysics, 64, 1429–1437.

Beltrão, J. F., J. B. C. Silva, and J. C. Costa, 1991, Robust polynomial fitting for regional gravity estimation: Geophysics, 56, 80-89.

Bruhn, C. H. L., and M. A. S. Moraes, 1989, Turbidites of the Urucutuca Formation, Almada Basin, Brazil: a field-laboratory for the study at channelized reservoirs. Bol. Geoc. Petrobrás, 3, 235-267.

Netto, A. S. T., and C. P. Sanches, 1991, Roteiro geológico da bacia do Almada, Bahia: Revista Brasileira de Geociências, 21, 186-198.

Ponte F.C., Asmus, H.E., 1978. Geological framework of the Brazilian continental margin.Geologis che Rundschau 68, 201–235

Acknowledgments

This work was supported by the Edital Universal by CNPq under contract No. 472229/03-6. We thank the technologists Emanuele F. La Terra and Carlos R. Germano and the student Suzanna C. Calache for their contribution to the gravity data survey. We also thank the Observatório Nacional for logistic support of the gravity data acquisition. P.T.L.M. was supported by fellowship from Prociência-UERJ. V.C.F.B and J.B.C.S. were supported in this research by fellowships from CNPq. Additional support for V.C.F.B and J.B.C.S. was provided by CNPq under contracts: No. 505265/2004-4 and No. 504419/2004-8. One of the authors (V.C.F.B.) was also supported by FAPERJ (contract No. E-26/170.733/2004).

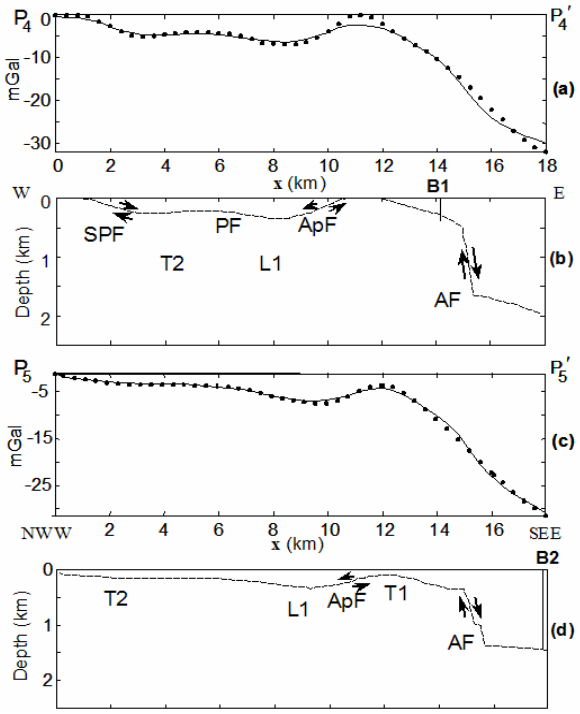

Figure 9 – Profiles $P_4P'_4$ and $P_5P'_5$. (a) Observed (dots) and fitted (solid line) Bouguer anomalies using weighted smoothness inversion along profile $P_4P'_4$ whose location is shown in Figure 3. (b) Estimated Almada basement relief along profile $P_4P'_4$ using weighted smoothness inversion (dashed line). (c) Observed (dots) and fitted (solid line) Bouguer anomalies using weighted smoothness inversion along profile $P_5P'_5$ whose location is shown in Figure 6. (d) Estimated Almada basement relief along profile $P_4P'_4$ using weighted smoothness inversion (dashed line). Basement depths provided from boreholes B1 and B2 were used as constraints in the inversions of the gravity anomalies profiles $P_4P'_4$and $P_5P'_5$, respectively. SPF – Serra Pilheira Fault; ApF - Apipique Fault; PF – Piábas Fault; AF – Arituaguá Fault; L1 – structural low; T1 and T2 – terraces.